USE PROCESS ANALYSIS TO ASSESS PREDICTED OZONE FORMATION IN THE UNITED ARAB EMIRATES

Yadong Xu

A Master's technical report submitted to the faculty of the University of North Carolina at Chapel Hill in partial fulfillment of the requirements for the degree of Master of Science in Environmental Engineering (MSEE) in the department of Environmental Sciences and Engineering.

Chapel Hill
2011

Approved by:

Dr. William Vizuete

Dr. Jason West

Dr. Sarav Arunachalam

ABSTRACT

YADONG XU: Use Process Analysis to Assess Predicted Ozone Formation in the United Arab Emirates
(Under the direction of William Vizuete)

We used the Community Multiscale Air Quality (CMAQ) model simulation to study ozone formation in the United Arab Emirates. Model performance evaluation results indicate severe over-prediction of O_3 and under-prediction of NO_2 especially in the Abu Dhabi urban region with a normalized mean bias (NMB) for O_3 at 179% and NO_2 at -64% at urban monitoring site KHAF. We used the process analysis tools together with a postprocessor tool pyPA to investigate the possible factors causing the poor performance and assess potential major contributors to high ozone episodes in the model. The results indicate that the local photochemical production and advection processes were the main contributors to surface ozone in the UAE.

We conducted two sensitivity runs in which NOx emissions are increased to understand model responses to different emission scenarios. Compared with the original model simulation, increasing the anthropogenic NOx emission rates by a factor of 6 in the Abu Dhabi urban region (the sensitivity run s2) caused significant predicted O_3 decrease by up to 80 ppb. The system switched from NOx-limited condition in the original model run to NOx-inhibited condition in the sensitivity run s2.

TABLE OF CONTENTS

LIST OF TABLES

Table

LIST OF FIGURES

Figure

LIST OF ABBREVIATIONS

ALD2	Acetaldehyde
ALDx	Propionaldehyde and higher aldehydes
CAMx	Comprehensive Air Quality Model with extensions
CMAQ	Community Multiscale Air Quality Model
ETH	Ethene
ETHA	Ethane
IOLE	Internal olefin carbon bond
ISOP	Isoprene
NMB	Normalized Mean Bias
NME	Normalized Mean Error
NOx	Oxides of nitrogen
PAR	Paraffin carbon bond
PEC	Primary elemental carbon
POC	Primary organic aerosol carbon
OLE	Terminal olefin carbon bond
ROOH	Higher organic peroxide
SMOKE	Sparse Matrix Operator Kernel Emissions System
TERP	Terpene
TOL	Toluene
VOC	Volatile Organic Compounds
WRF	Weather Research Forecast Model
XYL	Xylene

CHAPTER I

INTRODUCTION

The United Arab Emirates (UAE) is among the most rapidly growing nations in the world resulting in large increases in population, energy use, and vehicle traffic[1]. The UAE is also home to several large industries, and two international urban centers (Abu Dhabi and Dubai) with large vehicular sources of emissions and problems of traffic congestion. Large emissions of oxides of nitrogen (NOx) from vehicles and power plants are in proximity to potentially large emissions of volatile organic compounds (VOCs) from the petroleum industry. The climate in the UAE, in combination with these rapidly growing emissions, results in an environment conducive for high ozone production. Surface level ozone is an important air pollutant for its harm to people and the environment and this unprecedented growth in emissions poses important challenges for air quality management [2, 3].

Some of the first modeling of ozone in the region came from a global scale air quality model (AQM). In 2001, these global chemistry models predicted a summer time O_3 maximum over the Middle East, with mean mixing ratios in the middle and upper troposphere in excess of 80 ppbv [4, 5]. Other studies of the Arabian Gulf region, using global models, have also predicted relatively high concentrations of ozone [6]. These models have predicted impacts on air quality in the UAE from the long-range transport of air pollutants from Europe, and other regions of the Middle East [7-9]. Due to the large populations in the Middle East and North Africa, Duncan et al. (2008) estimated that European pollution causes more premature ozone-related mortalities in these regions than in Europe itself. The large influence of European emissions and its impact on

mortality are supported by other global modeling studies in the literature [8-10]. Each of these studies highlights the importance of regional transport of ozone into the region.

A limited number of regional scale modeling studies have been performed over the Middle East [11, 12]. The UAE Air Force and Air Defense Meteorological Department used their implementation of the Weather Research Forecasting (WRF) and developed an air quality forecasting system using WRF-Chem. Some of the greatest hurdles for completing this effort were the lack of accurate local emissions data in the Middle East [13, 14]. Nevertheless, the authors reported reasonable model performance for ozone concentrations, when compared with surface observations. Time series provided in the report, however, did show underpredictions of surface ozone at a surface monitor in the city of Gayathi. In another study, a regional scale application of the Comprehensive Air quality Model with extensions (CAMx) that focused on Qatar was developed, and included all of the UAE within the modeling domain [15]. Predictions of ozone from this model also showed an underprediction when compared to surface observations. The authors list as probable causes the lack of detailed emission data for the region, and the improper simulation of transport into Qatar. These authors point out that the model predicted large regional contributions to ozone concentrations and saw ozone transport over distances of 100-200 km per day. These studies highlight the difficulty in predicting ozone concentrations, the importance of regional transport of ozone, and the inaccuracy in the existing emission inventories.

Recognizing the importance of understanding the air pollution burden in the UAE, we used a state of the science regional scale air quality model to predict air pollutant concentrations for ozone, particulate matter and a few air toxics. As part of these efforts meteorological and emission inventory data using the most current global and local scale databases were developed. Although this study uses the best available information,

there are important uncertainties in our model results. This study will identify these uncertainties through detailed model performance evaluations using surface observational data. Our goal was to identify poor model performance and recommend future work to help improve model accuracy. Since the ultimate use of this modeling system is to support future policy decisions we have focused our analysis on high ozone events and on the highly populated urban area of Abu Dhabi.

CHAPTER II

METHODS

Air Quality Model

For this study the Community Multiscale Air Quality Model (CMAQ) was chosen. CMAQ is a comprehensive, three-dimensional, multipollutant, multiscale atmospheric chemistry, transport, and deposition model that has been developed by the U.S. EPA [16, 17] in collaboration with developers world-wide. CMAQ is a publicly available Eulerian grid-based model that can address tropospheric ozone, acid deposition, visibility, fine particulates, air toxics, and other air pollutant issues in the context of a “one atmosphere” perspective where complex interactions between atmospheric pollutants and regional-to-urban-scale circulations are simultaneously addressed.

For the CMAQ model we chose the Carbon Bond 2005 chemical mechanism (CB05) with chlorine updates [18], treatment of mercury chemistry and a few air toxics (formaldehyde, acetaldehyde and benzene), and Version 5 of the aerosol module. The CB05 mechanism is an update on the Carbon Bond IV chemical mechanism [19] that has been used in air quality models for several decades. The reactive chlorine chemistry mechanism is important to model the impact of Chlorine and/or HOCl emissions on oxidant formation and VOC decay rates. Chlorine chemistry may be important for the Arabian Gulf region since the study area includes substantial coastlines, which are an important source of chlorine emissions from sea-salt aerosols.

Due to the importance of international emissions over a large area on air quality in the UAE, we have selected a large model domain for these simulations that includes the entire Arabian Peninsula and portions of North Africa, Europe, Central Asia and India as shown in Figure 1. While this large domain captures the large-scale transport of pollutants, a nested smaller domain provides greater resolution in the immediate vicinity of the UAE. The large domain has a resolution of 36-km and 148 columns and 134 rows of grid-cells. The nested small domain has a resolution of 12-km and includes 78 columns and 72 rows of grid-cells. Each of the two domains has 34 vertical sigma levels with denser layers near the surface and fewer layers close to the top of the domain. The lowest layer is about 40 m thick.

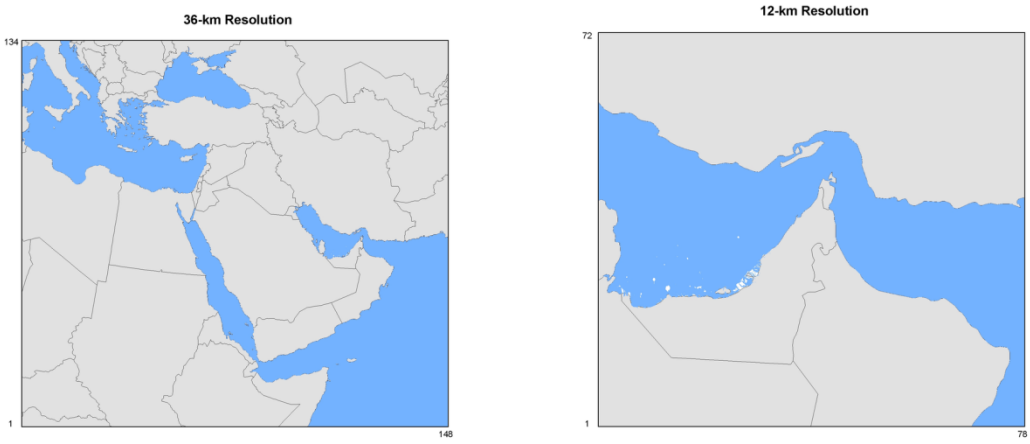

Figure 1 Maps of modeling domains used in CMAQ simulations showing the (a) outer domain at 36-km horizontal resolution and (b) the inner domain at 12-km horizontal resolution. Column and row extrema for each domain are indicated respectively at the ends of the southern and western boundaries.

We have chosen to model two episodes, one in the summer of 2007 (May 15 to August 31) and the second in the winter of 2007-2008 (Dec 15, 2007 to March 31, 2008), to capture two distinct seasons. All of the meteorological, emissions, and air quality modeling are performed over these two spatial domains and time frame. In our study, we focused the model performance evaluation on the summer episode because the

observed and modeled ozone for the winter episode were much lower than the ones in the summer episode.

The Weather Research Forecast (WRF) model, WRF V3.0.1, was used to generate the gridded meteorological input data for CMAQ [20]. The WRF Version 3.0.1 system is a Eulerian non-hydrostatic model consisting of microphysical processes of cloud and precipitation, longwave and shortwave radiative schemes, atmospheric turbulence and diffusion, a surface layer and soil layer parameterization scheme and a planetary boundary layer (PBL) scheme [21].

The Sparse Matrix Operator Kernel Emissions (SMOKE) system, SMOKE v2.4, was used to process the emissions input data. The input data for SMOKE were compiled from several global, regional, and local databases to create a temporally resolved and spatially distributed emissions data for CMAQ. The anthropogenic emissions were processed from a combination of several available database of the Climate Change and Impact Research, including The Mediterranean Environment (CIRCE) year 2005 country-level inventory, the Emissions Data for Global Atmospheric Research (EDGAR) year 2000 country-level inventory, the European Monitoring and Evaluation Program (EMEP) year 2006 50-km gridded inventory and a year 2004 point source inventory for industrial sources in Abu Dhabi, UAE. The biogenic emissions were estimated from the Model of Emissions of Gases and Aerosols from Nature (MEGAN) version 2.04 [22]. These represent the best efforts to process emissions for the region. The evaluation of uncertainties and known data gaps are described elsewhere [22].

To assist in the model performance evaluation, and provide additional insight on simulated ozone formation, we quantified the relative contributions of all predicted physical and chemical process rates. This was accomplished by using process analysis (PA) tools available in the CMAQ model. When Integrated Process Rate (IPR) and Integrated Reaction Rate (IRR) extensions are enabled during the CMAQ model run, the

concentration change for a certain chemical species caused by physical and chemical processes is described in mass conservation equations. By solving these equations, CMAQ can output large and complex datasets extracting the process details for each species in each grid cell. It is a useful analytical tool widely used to understand and quantify physical and chemical processes of ozone formation[23-25]. A postprocessor called pyPA is used to aggregate process analysis rates for a user-defined collection of grid cells. For this collection of cells, the concentration changes and individual process rates can be quantified at each time step. The pyPA postprocessor can be used to analyze a fixed region at the location of interest and follow the vertical evolution of the PBL. It also has the flexibility to characterize a moving volume such as an ozone plume that may have formed in the model.

Surface Measurements

For ground-based measurements we relied on data from the Environment Agency – Abu Dhabi (EAD) air quality monitoring network whose locations are shown in Figure 2a and Figure 2b, and pertinent information in Table 1. To help evaluate model performance in Europe we relied on surface stations within the European Monitoring and Evaluation Programmme (EMEP) [26].

Among the 10 EAD air quality-monitoring stations, only the observational data collected at 6 sites were considered suitable for model evaluations: ALSC, BIDA, BANI, GAYA, and LIWA, KHAF. Among these 6 sites, the Al Ain Institute site (ALSC) represents a residential area near the city of Al Ain; the Bida Zayed (BIDA) site is located in an open area close to the village of Bida Zayed; The Baniyas station (BANI) is placed in the northwest corner of the Saad Bin Obadah Primary school in the urban residential Baniyas area with open surroundings; The Gayathi station (GAYA) is representative for a small residential town, about 30-km south of the Ruwais industrial area; The Liwa oasis (LIWA) station located in a remote place without local sources of

pollution; The site at the Khalifa school (KHAF) is a typical urban site located in the Mishrif area with no major roads or industry in the vicinity of the monitoring station. The remaining four monitoring sites were influenced by local sources and considered to have poor representativeness at the resolution of the models. For example, the site at Khadejah school (KADJ), located at the downtown area of Abu Dhabi, is surrounded by heavy traffic; the site at Hamdan street (HAMD) is located right besides an urban main road; the site at Mussafah (MUSA) is located in an industrial zone, heavily affected by the local industry. Although useful for characterizing microenvironments, these measurements were not suitable to evaluate model performance and were not included in this analysis. Unusually low values were recorded at BIDA throughout the months of July and August 2007, leading to a possibility of instrument problems at the site; thus data from this site were removed in the subsequently quality-assured datasets provided by EAD; similarly data from LIWA were removed for March 2008.

Figure 2a. The location of the surface monitors maintained by the Environmental Agency Abu Dhabi. Descriptions of monitors are shown in Table 1.

Figure 2b. The location of the surface monitors maintained by the Environmental Agency Abu Dhabi located in Abu Dhabi urban region.

Abbrev.	Air Quality Monitoring Station	Type of Station	Location of grid cells in 12km domain (Column, Row)
ALSC	Al Ain Islamic Institute	SubUrban/Residential	39, 27
KADJ	Khadejah School	Downtown	28, 28
KHAF	Khalifa School	SubUrban/Residential	28, 28
GAYA	Gayathi School	Small Downtown	15, 21
BIDA	Bida Zayed	Urban/Residential	23, 20
BANI	Baniyas School	SubUrban/Residential	30, 27
HAMD	Hamdan Street	Urban Roadside	28, 28
ALST	Al Ain Street	Roadside	40, 27
MUSA	Mussafah	Industrial	29, 27
LIWA	Liwa Oasis	Regional Background	22, 15

Table 1 EAD Air Monitoring Stations: Representation Type and Grid cell location

CHAPTER III

RESULTS

Before the results from this CMAQ simulation can be used for future air quality planning, its performance for baseline conditions must be evaluated by comparing its outputs against ambient observations. The following sections describe these efforts, focusing on urban and rural areas of the UAE during high ozone episodes.

Model Performance Overview for All Sites

We followed U.S. EPA's guidance [27] to evaluate model performance for ozone and NO_2 against routine surface measurements. Predictions made at the 36-km and 12-km grid resolution were compared to the EAD surface measurements. This included calculation of NMB (Normalized Mean Bias) and NME (Normalized Mean Error) as shown in equations (Equation 1 and Equation 2). Table 2 shows the NMB and NME for ozone and NO_2 predictions made at the 36-km and 12-km grid cell resolutions at the monitoring sites in UAE for the summer episode. At the 12-km grid resolution, ozone was over-predicted with a NMB of 178.8% and NME of 188.5% at KHAF site, while NO_2 was under-predicted with a NMB of -64.2% and a NME of 79% at this site. The LIWA monitor had the best agreement of NO_2 and O_3 among all the sites with a O_3 NMB of 22.1% and NO_2 NMB of -6.2%.

$$NMB = \left[\frac{\sum_1^N (Model - Obs)}{\sum_1^N Obs}\right] \times 100\% \quad (1)$$

$$NME = \left[\frac{\sum_1^N |Model - Obs|}{\sum_1^N Obs}\right] \times 100\% \quad (2)$$

Resolution	36-km		12-km		36-km		12-km	
UAE_Site_ID	NMB_O_3 (%)	NMB_NO_2 (%)	NMB_O_3 (%)	NMB_NO_2 (%)	NME_O_3 (%)	NME_NO_2 (%)	NME_O_3 (%)	NME_NO_2 (%)
ALSC	220.82	-73.11	224.49	-89.18	221.26	74.08	224.81	89.28
BANI	79.4	'N/A'	58.18	'N/A'	80.69	'N/A'	63.53	'N/A'
GAYA	53.58	-64.4	49.56	-70.02	54.49	68.26	51.27	76.45
KHAF	206.66	-49.15	178.82	-64.16	212.93	68.13	188.46	78.96
LIWA	22.78	-31.2	22.06	-6.17	26.61	56.01	26.44	64.22

Table 2 Normalized mean bias (NMB) and normalized mean error (NME) of O_3 and NO_2 at the air monitoring stations for the summer episode.
Note: 'N/A' means 'not applicable'. No statistic evaluation of NO_2 at BANI site because of lack of NO_2 observations.

European monitors in the coarser 36-km grid showed better model performance with the O_3 NMB of 23% and O_3 NME of 49%. In contrast, UAE monitors in the 36-km grid simulation showed poor model performance with the O_3 NMB of 90% and the O_3 NME of 95%.

Detailed Model Performance Evaluation and Process Analysis Results for Urban Site KHAF

To understand these large biases we focused our study on measurements made in the city of Abu Dhabi. Abu Dhabi has the highest population density in the Abu Dhabi emirate and thus it is critical to understand the large biases found there. In central Abu Dhabi, the KHAF monitor has been identified to best represent the urban area overall since it is not near any major highway sources as shown in Figure 2b. Based on observational data from KHAF we noted that the month of July had the highest

measured ozone concentrations for the year of 64 ppb. Figure 3 shows the daily early morning (6:00-9:00 LST), and late night (2:00-5:00 LST) average observed and modeled concentrations of O_3 and NO_2 at KHAF for each day in July 2007, along with the bias and error statistics. These temporally aggregated data were used to examine the model behaviors throughout the diurnal ozone cycle[28, 29]. At KHAF, modeled NO_2 concentrations during early morning hours had a consistent bias of around -15 ppb, which continues in the late night periods. CMAQ overpredicted O_3 during most of the month at KHAF with biases up to 100 ppb. The only exception to this bias was on July 26 when the average bias of the modeled and observed NO_2 concentrations were within -5.0 ppb and the average ozone bias were within 12.5 ppb.

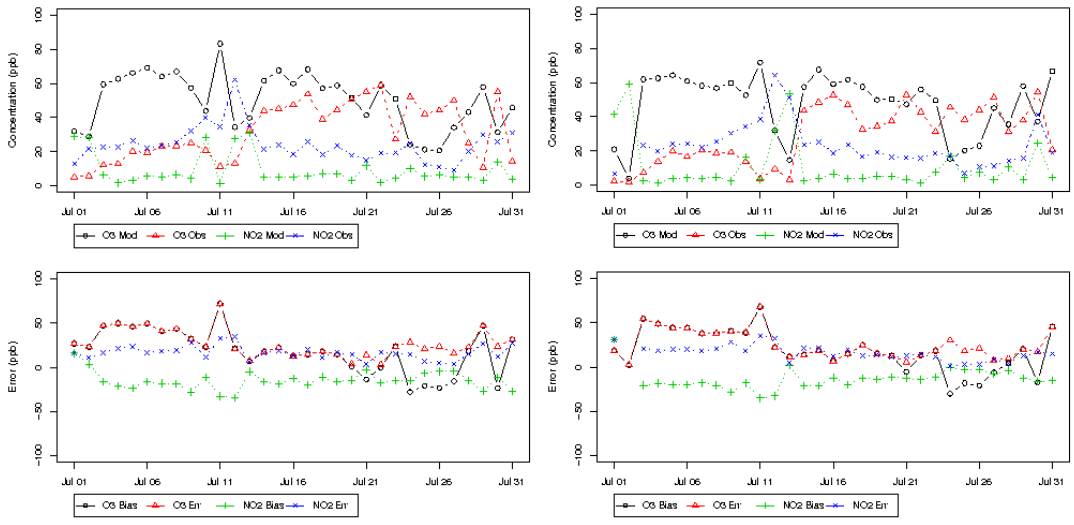

Figure 3 Early morning (6:00-9:00 LST) (left panel) and late night (2:00 - 5:00 LST) (right panel) O_3 and NO_2 averaged concentrations at KHAF for July 2007.

On July 3, 2007, the highest bias of 100 ppb between the modeled and observed ozone concentration occurred at the KHAF site. The time series plots in Figure 4 show the hourly averaged concentrations predicted by the model (red dashed lines), and measured by the KHAF surface monitor for ozone (solid red lines). Surface ozone concentrations were over-predicted and observed NO_2 concentrations (showed in solid

blue lines) were under-predicted for most hours of the day at the KHAF site. Figure 4 shows the wind direction and speed predicted by the model and observed at the monitors. The model failed to capture the wind directions in the morning and the wind speeds in the afternoon were over-predicted at KHAF site. In our analysis, we found that on nearly every high ozone day, there exhibited a rotational wind (wind directions changing gradually in a circular pattern from morning to night) similar to what was shown in Figure 4. Although the model is able to represent a circular pattern, it does not capture the magnitude and timing of directional changes. The model predicted planetary boundary layer (PBL) heights at the KHAF coastal site of less than 500 meters for this day, as shown in Figure 4. This is generally less than the peaks of over 2500 meters found at the inland sites. Inspection of this grid cell shows that 20% is water, and this modeled land-cover could be influencing these PBL heights.

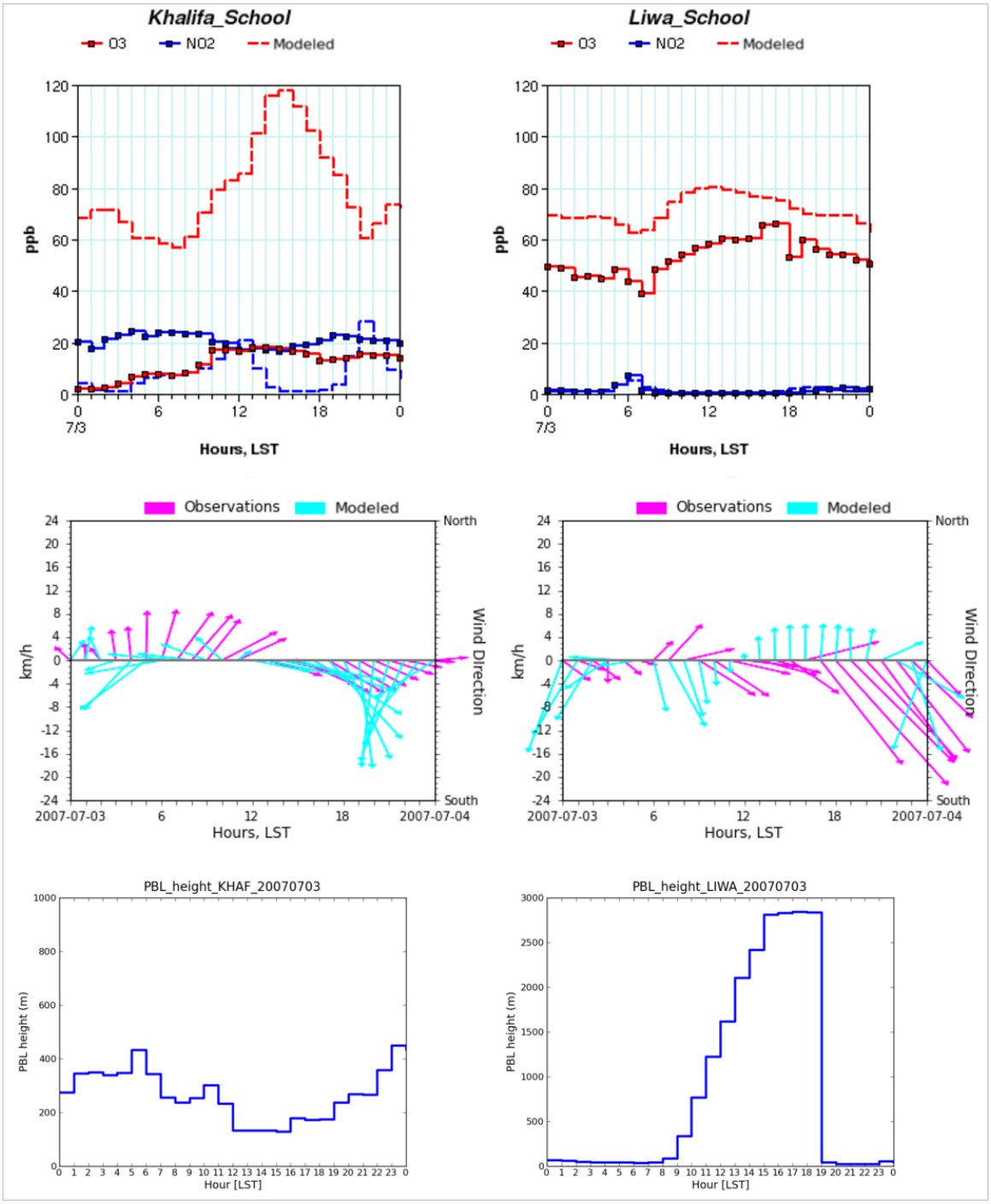

Figure 4 Time series plots for O3 and NO2, the dashed red line shows O3 modeled concentrations, the solid red line shows O3 observed concentrations, the dashed blue line shows NO2 modeled concentrations, the solid blue line shows NO2 observed concentrations (top); Wind vector plots, the purple color shows the observations and the blue color shows the modeled. (middle) and PBL height (bottom) for KHAF (left panel) and LIWA (right panel) sites on July 03, 2007.

Process analysis (PA) was conducted on July 3, 2007 with all chemical and physical processes calculated for a single horizontal grid cell containing the KHAF monitoring site. Vertically, the PA volume followed the hourly PBL change. At the KHAF grid cell, ozone concentrations peaked at 115 ppb at 15:00 LST, nearly 100 ppb higher than the measured value. In the model the advection and chemistry were the largest processes rates increasing ozone concentrations. Photochemical process rates were the major contributor to the diurnal change of the ozone concentration with rates as high as 16.1 ppb/hour. For the photochemical day, from 9:00-17:00 LST, chemistry played a positive role for ozone formation, with 72% contribution among all the processes. The predicted NO_2 concentrations were much lower than the observations for most hours of the day except for two peaks that occurred around 11:00 LST and 22:00 LST in the model. Chemistry and advection are also the major contributors for the diurnal change of NOx at this site, with chemistry playing a negative role consuming NOx. The PA results also showed that NO and NO_2 emission rates at this site were zero (Table 3). This indicates further investigation on the NOx emissions is needed at this site.

Species	Processes	Peak ppb/hour	Fractions*	Net effect*
O3	Chemistry	16.1	72%	Positive
	Advection	14.8	6.9%	Positive
NO	Chemistry	14.3	56%	Negative
	Advection	9.7	38.5%	Positive
	Emission	0	0	--
NO2	Chemistry	11.1	27.1%	Negative
	Advection	13.7	36.5%	Negative
	Emission	0	0	--

Table 3 Summary of the process analysis results at KHAF for July 03, 2007
*: Fractions and net effect only calculated for the hours of the photochemical day (9:00 LST – 17:00 LST)

To further investigate whether the ozone formation in this PA volume was under NOx-limited or NOx-inhibited conditions, we used process analysis results from the PA volume to calculate the ratio of peroxide (H_2O_2 + ROOH) production to nitric acid (HNO_3) production, also called the Sillman ratio. A Sillman ratio greater than 0.5 indicates that ozone was formed under NOx-limited conditions. A Sillman ratio less than 0.5 indicates that the system is under NOx-inhibited condition [30, 31]. Our results show the Sillman ratio at KHAF site on this day started to rise rapidly after 14:00 LST, reaching a peak Sillman ratio of 3.8 at 16:00 LST (Figure 5). This indicates O_3 was made under NOx-limited conditions in the model.

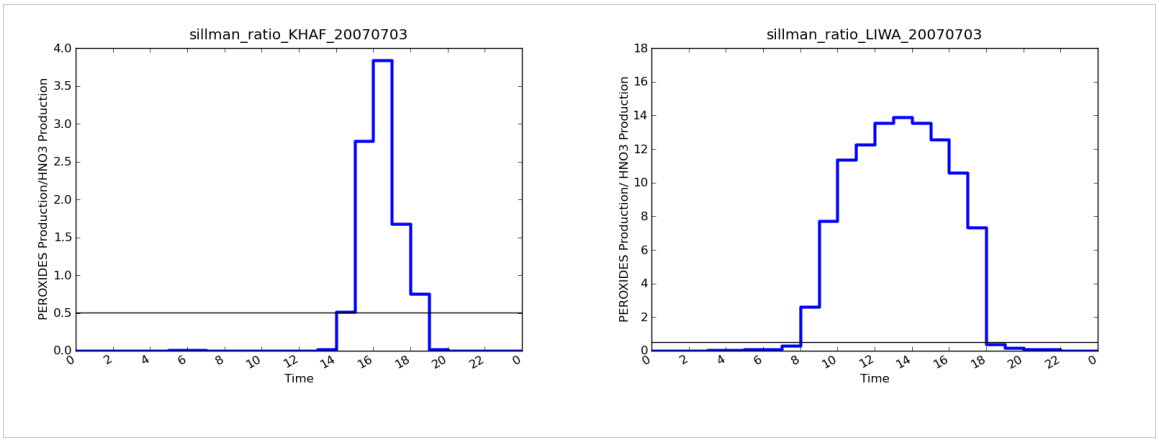

Fig.5 Sillman ratio for KHAF and LIWA sites on July 03, 2007 in the original model run.

Detailed Model Performance Evaluation and Process Analysis Results for Rural Site LIWA

The LIWA monitor is located in the Liwa oasis outside the urban area of Abu Dhabi, has less local sources of pollution, and could be considered representative of regional background. This makes this site ideal for understanding the impact of pollution from Abu Dhabi, and for evaluation of model performance for background concentrations. Comparisons of O_3 at LIWA show modeled concentrations that agreed well with the observed data within 20 ppb as shown in Figure 6. The observed NO_2

concentrations are generally low at all hours with the model able to predict observed concentrations. . The model also predicted a 40 ppb decrease in ozone concentrations in the last week of July 2007, and a subsequent increase on the last day of July.

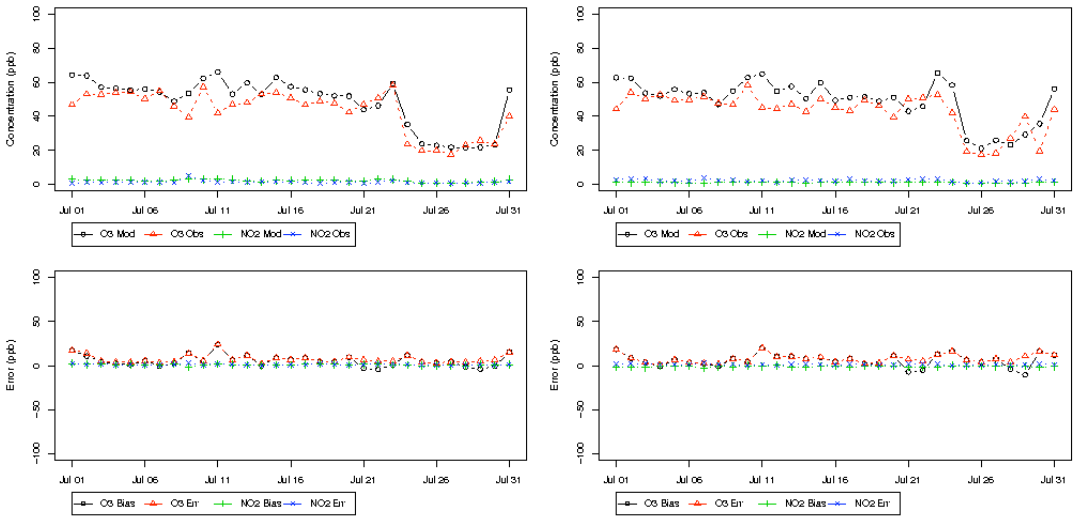

Figure 6 Early morning (6:00 – 9:00 LST) (Left) and late night (2:00 – 5:00 LST) (Right) O_3 and NO_2 concentrations at LIWA during July 2007.

The time series plots in Figure 4 show the hourly concentrations predicted by the model (dashed red lines), and measured by the LIWA surface monitor for ozone (solid red lines) on July 03, on this day the highest ozone bias occurred at KHAF site. In contrast to the KHAF monitor, the LIWA monitor indicated relatively smaller ozone bias between the modeled and observed concentrations with differences of up to 20 ppb. NO_2 concentrations were also better at LIWA, modeled within 2.0 ppb of observations. In the wind vector plots of LIWA in Figure 4, the model failed to capture the wind directions in most hours of the day and the wind speeds in the afternoon were under-predicted at this site. The PBL heights at the LIWA site are much higher than the KHAF site, with a peak of 2800 m, indicating that the pollutants are well-mixed in this region.

Based upon PA analysis, in contrast to the KHAF site, ozone photochemical processes played a less important role at LIWA site, with chemistry contributing 32.5%

to ozone. At the LIWA site, the process rates by chemistry peaked at only 2.8 ppb/hour, 13 ppb/hour less than the peak calculated at KHAF. The process rates for advection (including horizontal and vertical advection), entrainment (dominated by its vertical component) and dilution due to vertical entrainment are also much smaller than the ones at KHAF site. This caused the ozone concentration at this site to vary only between 65-80 ppb on this day. Local emission processes provided NO at a peak rate of 3.6 ppb/hr, but chemistry consumed it immediately (Table 4). The Sillman ratio at LIWA site on this day was also very different from the one at KHAF site, it started to rise much earlier, around 8:00 LST, reaching a peak Sillman ratio of 14 at 13:00 LST, which is much higher than the one of 3.8 at KHAF (Figure 5). This indicates O_3 was also made under NOx-limited conditions at this site.

Species	Processes	Peak ppb/hour	Fractions*	Net effect*
O3	Chemistry	2.8	32.5%	Positive
	Advection	3.6	15.8%	Negative
NO	Chemistry	3.2	33.8%	Negative
	Advection	0.46	2.8%	Negative
	Emission	3.6	49.5%	Positive
NO2	Chemistry	3.1	39.5%	Positive
	Advection	1.6	12.8%	Negative
	Emission	0.4	6.6%	Positive

Table 4 Summary of the process analysis results at LIWA for July 03, 2007
*: Fractions and net effect only calculated for the hours of the photochemical day (9:00 LST – 17:00 LST)

Detailed Model Performance Evaluation and Process Analysis Results for High Ozone Episodes

Critical for the effective use of regulatory models is model performance with regard to accurately reproducing high ozone episodes. In this analysis the process analysis tool was used to quantify model predicted processes most relevant to predicted high ozone episodes and provide guidance for further study. For this study we focused

on two simulation days: highest modeled 1-hour ozone concentration (July 01, 2007), and the highest observed 1-hour ozone concentration (July 22, 2007). Investigation of the day with the highest modeled 1-hour ozone concentration will help us gain understanding of how the high ozone concentrations were generated in the model. Furthermore, understanding the model's ability to reproduce the high observed 1-hour ozone concentrations would provide guidance on whether we can use the model results to effectively evaluate control policies.

Highest Predicted Ozone Day

On July 01, 2007, the model predicted the highest hourly ozone concentration during the entire summer episode. On this day, CMAQ predicted the formation of a plume of ozone at the coastal area between Abu Dhabi and Dubai around 10:00 LST with a peak of 149 ppb as shown in Figure 7. The plume moved slowly toward the ALSC monitoring site arriving at 20:00 LST. The arrival of this plume causes a 20 ppb increase in predicted ozone concentrations at the ALSC monitor. This sudden increase in ozone concentration, however, was not observed at this site. Ozone was over-predicted by up to 48 ppb throughout the whole day and NO_2 was under-predicted by up to 65 ppb at this site.

On this high ozone day, the model predicted an offshore breeze at 11:00 LST that lasted until 21:00 LST. At 10:00 LST, the model predicted an area of stagnation at the origin of the high ozone plume. The high ozone plume (with hourly concentrations greater than 120 ppb) is observed to move with wind direction changes. Through inspection of the O_3 spatial plots for the whole month of July, we found that this co-occurrence of the high ozone plume movement and the rotational wind patterns occurred 80% of the time when there was high ozone predicted.

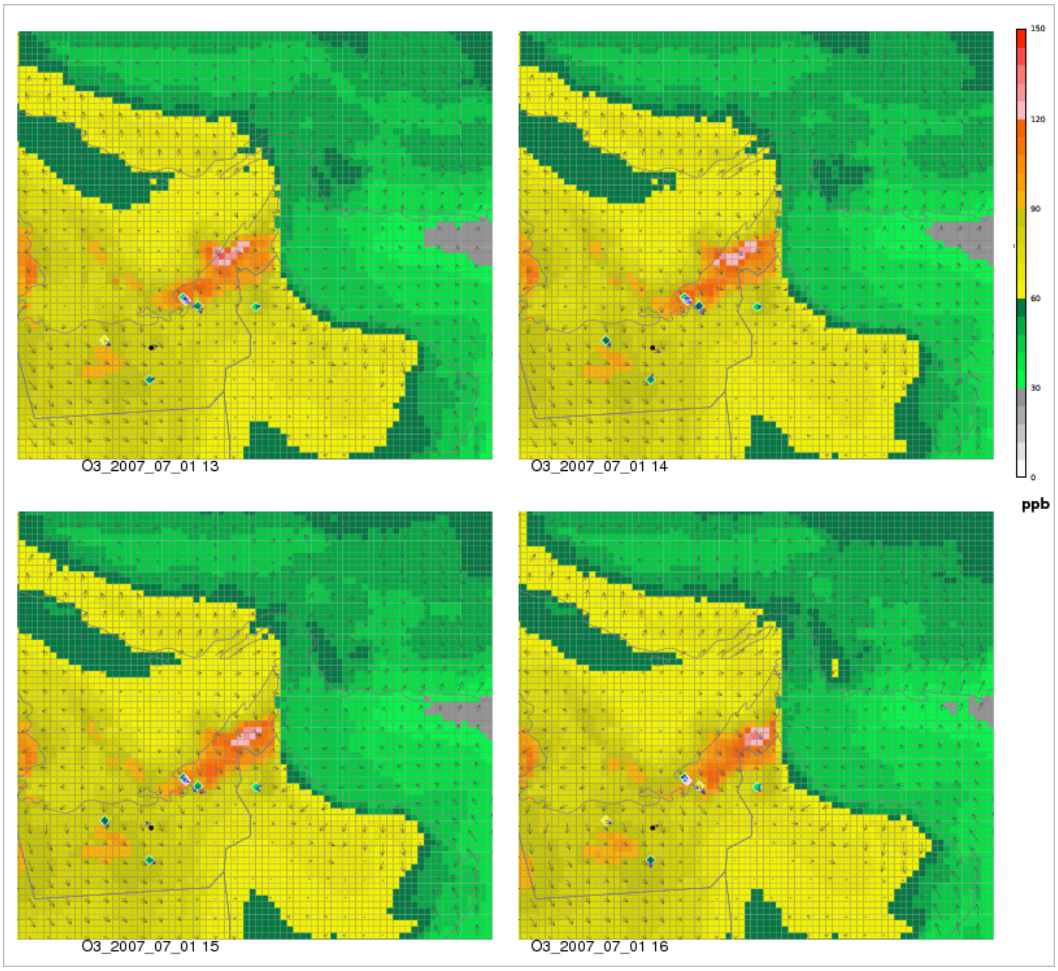

Figure 7 Spatial plots from hour 13:00 LST to 16:00 LST showing high ozone plume formed in-between Abu Dhabi and Dubai on July 01, 2007 in the model

To understand the relevant chemical and physical process rates that formed this plume we used process analysis output and the pyPA post processor to isolate the plume as it traveled from the northwest to the southeast, and finally arriving at Al Ain. The horizontal extent of our analysis includes the cells with ozone concentrations greater than 120 ppb following the ozone plume movement shown in Figure 7 for hours 13:00 – 16:00 LST. Vertically, we followed the hourly change in PBL. The PA data shows that ozone photochemical processes played a positive role during daytime (7:00 – 18:00 LST) in the plume. The peak chemical production rate for ozone reached 32 ppb/hour at

11:00 LST. Analysis of process rates that influence final NO concentrations in the plume shows that the NO emission rates (positive) and chemistry process rates (negative, indicating NO destruction) are out of phase with the same magnitude. This indicates that NO was consumed immediately after it was emitted. NO_2 was formed mainly by chemistry in the plume at early morning, and consumed by chemistry from 8:00 to 13:00 LST. In addition to chemical production, advection brought NO_2 from surrounding areas in the morning, which leads NO_2 concentration to reach a peak at 8:00 LST of 13 ppb. The Sillman ratio in the plume during the morning hours (before 11:00 LST) is lower than 0.5 and it increased rapidly to 1.73 at 11:00 LST and reached the peak of 3.28 at 14:00 LST. This indicates that the ozone plume switched from NOx-inhibited to NOx-limited around 11:00 LST as a result of the loss of NOx due to chemistry.

The NOx and VOC emissions at the area where the ozone plume occurred were found to be also higher than other regions across the domain. This further confirmed that the ozone plume is mainly formed by local chemistry. There is no surface observational data available at this region to prove or disprove the existence of this ozone plume. This indicates the need for more routine measurements at the region between these two cities, Abu Dhabi and Dubai.

Highest Observed Ozone Day

For regulatory purposes, the model must be able to replicate observed high ozone days. On July 22, 2007, the highest hourly ozone concentration in the entire modeling episode of 80 ppb was observed at 14:00 LST at the GAYA monitor site. The time series plot in Figure 8 shows the model predicted and measured hourly concentrations at this site, and wind vectors. At this site, the model performance for O_3 in the morning hours was within 20 ppb of observed values. The model however, failed to predict the 30 ppb drop in ozone concentrations after sunset at 19:00 LST resulting in an error of 60 ppb (Figure 8). At the time when the observed ozone peak occurred at this

site, the model over-predicted the ozone concentrations at other monitoring sites, especially ALSC (as in the spatial plots of Figure 8). There was a narrow ozone plume simulated in the model located between Abu Dhabi and Dubai. The meteorological performance on this day was also poor. Wind speeds at GAYA site were over-predicted during most of the hours of the day. The model failed to capture the observed transition in wind direction, with wind blowing toward north in the morning and rotating toward southeast in the afternoon.

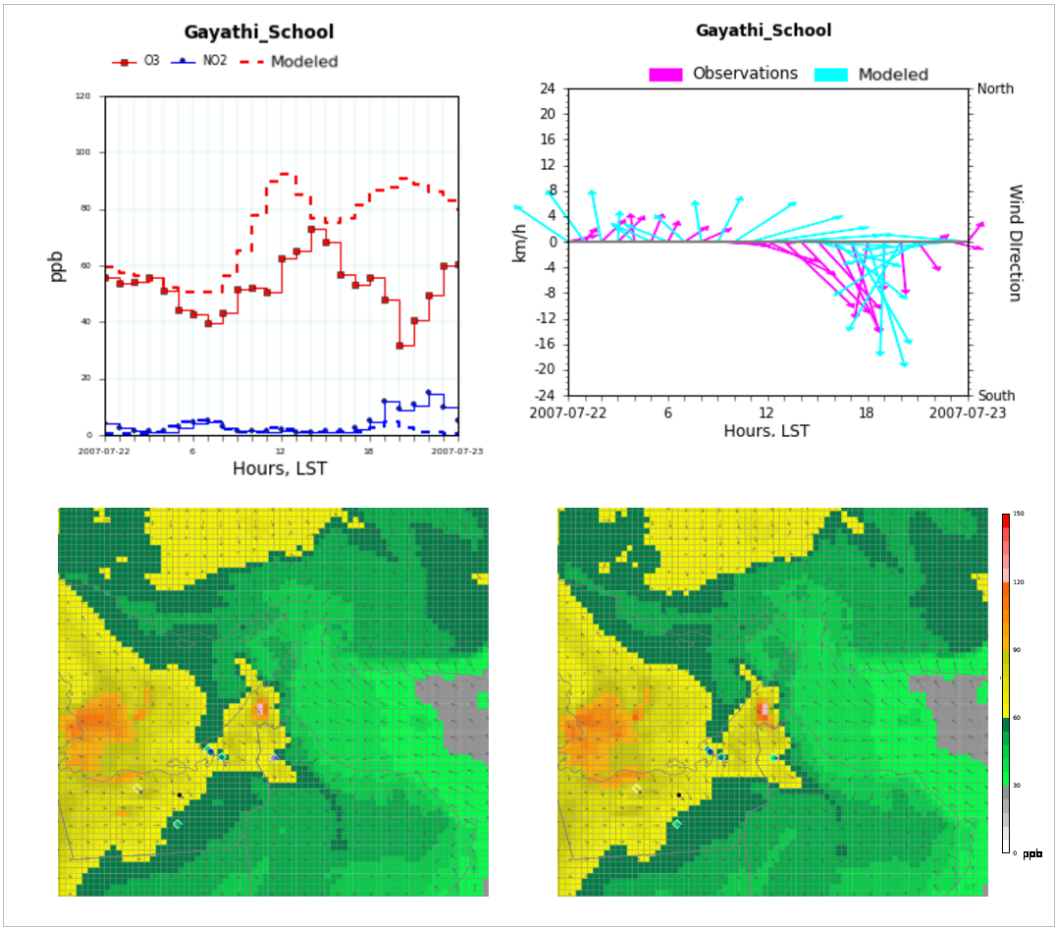

Figure 8 Upper-left : Time series plots for O3 and NO2, the dashed red line shows O3 modeled concentrations, the solid red line shows O3 observed concentrations, the dashed blue line shows NO2 modeled concentrations, the solid blue line shows NO2 observed concentrations; Upper-right : Wind vector plots, the purple color shows the observations and the blue color shows the modeled(upper right) and Ozone spatial plots (14:00 LST at the lower left and 15:00 LST at the lower right) for GAYA site on July 22, 2007.

Using process analysis output and the pyPA post processor, we calculated the chemical and physical processes influencing model predictions at the grid cell containing GAYA site. As in our previous analysis, the PA volume vertically followed the hourly PBL change. The calculated process rates for advection, entrainment, dilution, and detrainment rates contributed little to the net increase of ozone concentrations with rates of up to 5 ppb/hr. The chemical production process rate was the major contributor to ozone during daytime with rates up to 15 ppb/hr (8:00 – 5:00 LST). The increasing pattern and the magnitude of ozone concentrations agree well with the surface observations in the morning, which is corresponding to the agreements between the modeled and observed NO_2 during the same time period. The model failed to capture the NO_2 peak that occurred after 18:00 LST, which could be the reason that the modeled ozone concentrations did not show the drop in the late afternoon and evening time as was observed at this site.

These results indicate a model whose ozone production is sensitive to NOx concentrations. Physical processes had a relatively smaller impact on ozone concentrations, leaving chemical production rate as the major contributor.

NOx Emission Sensitivity

The model performance analysis indicates that the ozone formation in the model was under NOx limited conditions. To investigate the model sensitivity we increased NOx emissions in the model in two scenarios. In the first we added mobile emissions to downtown Abu Dhabi. We found in our analysis that NOx emission rates in the model at the cell containing KHAF site (row 28, column 28 in 12-km domain) were zero. The reason is because the UAE main roads, used as a spatial surrogate to process the country level emissions from mobile sources, stopped before it entered the cell (Figure 9). Not only NOx, other species related to the emissions from mobile sources, such as CO, and the various CB05 species for VOCs (such as PAR, ETH, ETHA, OLE, IOLE,

TOL, TERP, XYL), SO_2, had zero emissions in the model as well. This indicated that emissions from mobile sources in the cell containing KHAF site were missing.

A sensitivity scenario (labeled as s1) was created that copied emissions from the urban cell (row28*column 30) where 99% of the NOx and VOC emissions are from mobile sources. The emissions for all 22 species (NO, NO_2, CO, PAR, ETH, ETHA, OLE, IOLE, TOL, TERP, XYL, ALD_2, ALDX, SO_2, CH4, ACET_TOX, BENZ_TOX, UNR, POC, PEC, ISOP, NH3) related to mobile sources were added into KHAF cell and a CMAQ simulation was completed for the month of July.

The model simulation results for sensitivity run s1 showed that adding mobile sources emissions to the single cell containing KHAF site brought limited improvement on ozone model performance across the domain. Compared with the original model run, hourly O_3 concentrations decreased by up to 7.5 ppb at KHAF site, while the maximum increase of O_3 hourly concentration was within 2.0 ppb among the adjacent cells.

A second sensitivity scenario (labeled as s2) increased anthropogenic NOx emission rates by a factor of 6, for 7 grid-cells covering the Abu Dhabi urban region (Figure 9). This factor was estimated by fitting the predicted daytime peak NO_2 concentrations to the observed value on July 12 when the largest NO_2 bias occurred at KHAF site in the original model simulation. This resulted in increasing NOx emissions sources in these cells include area sources, mobile sources; the emissions from biomass burning and commercial shipping were kept the same as the ones in the original emission files. The modeling episode for this sensitivity run was the month of July as well.

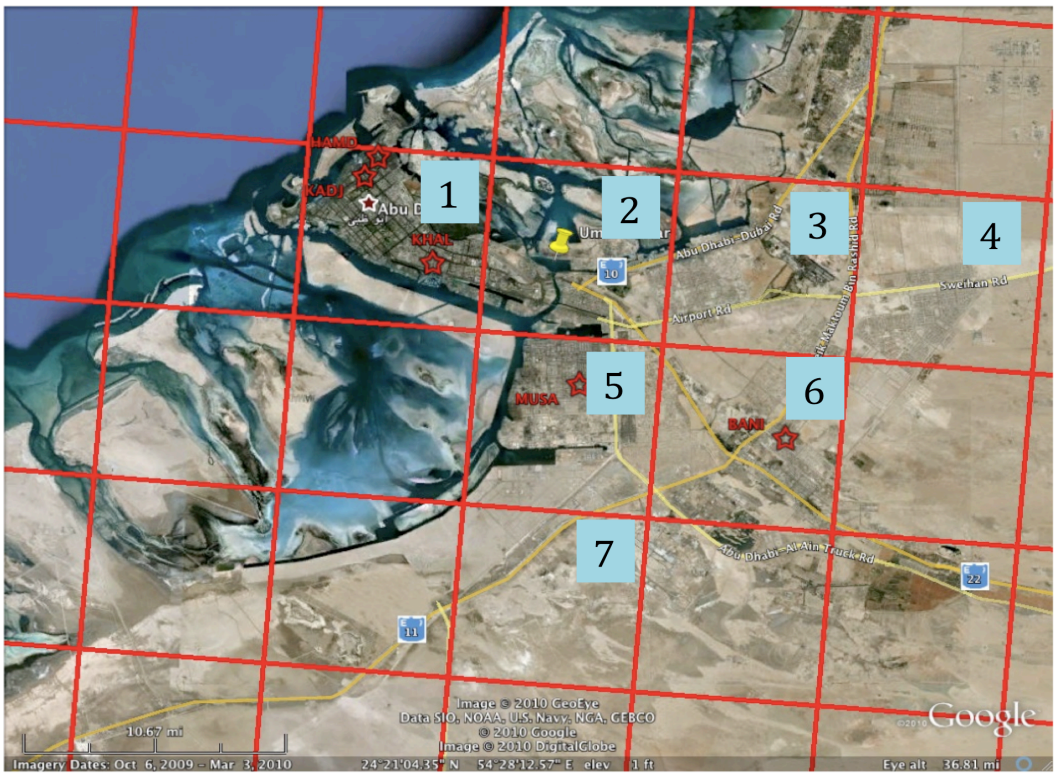

Fig.9: Abu Dhabi region overlaid by 12-km grids. In the sensitivity run s1, the emissions from the cell labeled as '3' in the original model run were copied into the cell labeled as '1', which contains the monitoring site KHAF. In the senstitivity run s2, the cells marked by '1' to '7' are the 7 cells selected to increase anthropogenic NOx emissions by a factor of 6.

The sensitivity run s2 brought significant changes in O_3 and NOx predictions in the Abu Dhabi region. Figure 10 shows the time series plot for the diurnal O_3 and NO_2 concentrations at KHAF site on July 03 in the original model simulation and the sensitivity run s2. As shown by the red line on the left panel of Figure 10, comparing the sensitivity run s2 to the original model simulation, O_3 predictions decreased up to 70 ppb. This day's modeled peak O_3 was still overpredicted, but the bias was 30 ppb lower than the one in the original model. During the early morning and afternoon (14:00 – 19:00 LST), O_3 was still severely over-predicted. Only for two short periods, around 11:00 LST and 20:00 LST, the predicted ozone in the sensitivity run s2 was lower than the observed. As showed by the red line of the right panel of Figure 10, NO_2 in the sensitivity run s2 was over-predicted for most of the hours of the day, in contrast to the

NO_2 under-prediction in the original model simulation. There is a temporal disagreement in the predicted and observed NO_2 concentrations: the observed NO_2 was fairly constant throughout the day, around 20 ppb. In s2, the predicted NO_2 concentrations in the simulations showed two peaks, one occurred around 11:00 LST and the other at 20:00 LST. This temporal disagreement could be attributed to the emission temporal profile, a typical North American urban emission temporal profile, used in the SMOKE processing, which likely does not reflect the real activities in UAE. For the entire month of July, the model performance for the sensitivity run s2 had a significant change for BANI site. O_3 was over-predicted at this site in the original run, while the O_3 predictions in the sensitivity run s2 show a much better agreement with the observed O_3 at this site (Figure 11). The overall model performance for the sensitivity run s2 at KHAF site was slightly better than the one in the original model simulation.

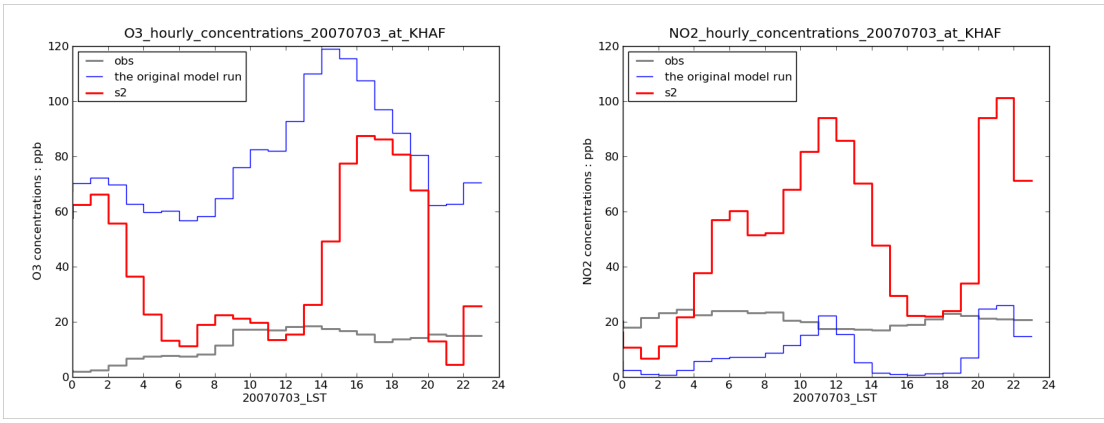

Fig.10: Time series plots for the sensitivity runs s2 compared with the observations and the original model run: O_3 hourly concentrations (left panel) and NO_2 hourly concentrations (right panel). The grey line shows the observations, the blue line shows the results from the original model simulation, and the red line shows the results from the sensitivity run s2.

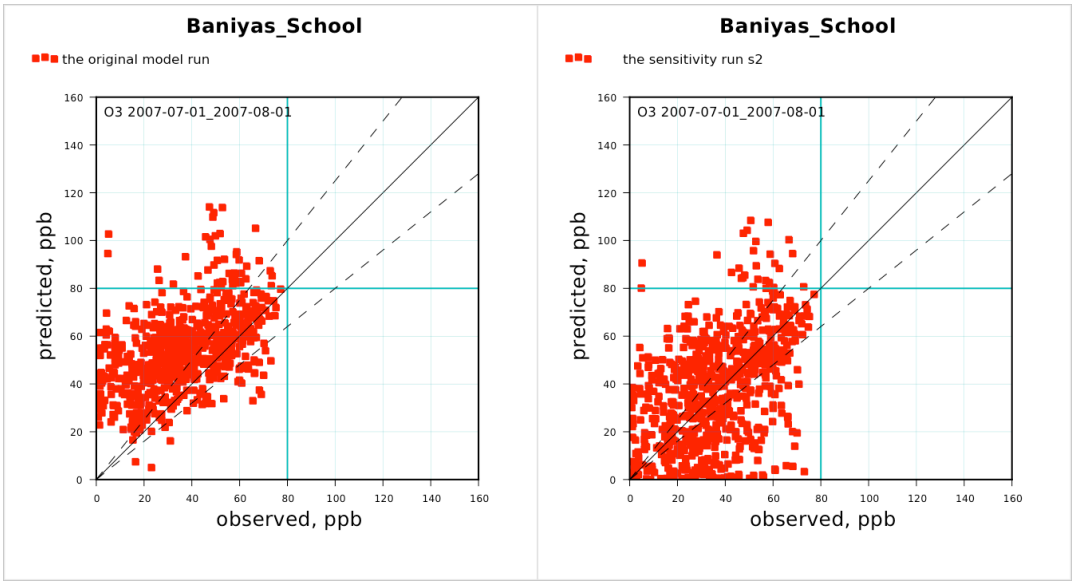

Fig.11: O3 scatter plots for the original model run (left panel) and the sensitivity run s2 (right panel) for the month of July at BANI site. The predicted hourly ozone concentrations are at y-axis and the observed hourly ozone concentrations are at x-axis.

Process analysis was also performed on the new NOx emission sensitivity model run s2 for KHAF site on July 03, 2007. Ozone diurnal variations in concentrations changed significantly. With more NOx in the system, the predicted hourly ozone concentrations were much lower than the one in the original model simulation, leading to a lower ozone bias between the predictions and the surface observations. Compared to the process analysis results for the original model simulation, both physical and chemical process rates are much higher in s2, with a peak advection process rate of 118.6 ppb/hour positively contributing to ozone formation at KHAF site, indicating more O_3 production in adjacent cells being advected into this cell. Photochemical process is still a major contributor to the ozone change. In contrast to the mainly positive contribution in the original model simulation, chemistry contributed negatively to ozone formation in the sensitivity run s2 (Table 5). This can be attributed to more NO in the system titrating O_3 in this region.

Species	Processes	Peak ppb/hour	Fractions*	Net effect*
O3	Chemistry	151.0	33.3%	Negative
	Advection	118.6	57.2%	Positive
NO	Chemistry	152.1	46.4%	Negative
	Advection	133.3	3.7%	Negative
	Emission	133.8	29.1%	Positive
NO2	Chemistry	152.5	32.6%	Positive
	Advection	113.8	48.6%	Negative
	Emission	14.8	2.8%	Positive

Table 5 Summary of the process analysis results for the sensitivity run s2 at KHAF for July 03, 2007
*: Fractions and net effect only calculated for the hours of the photochemical day (9:00 LST – 17:00 LST)

The peak concentrations for NO and NO_2 in the PA volume containing KHAF site in the sensitivity run s2 increased significantly by 100 ppb and 70 ppb respectively. The NO_2 concentrations at KHAF site for the original run were much lower than the observed ones for most of the hours on this day, while the NO_2 concentrations in the sensitivity run s2 were up to 80 ppb higher than the observations for most of hours of the day. The model still could not capture the higher observed NO_2 concentrations between 0:00 LST to 4:00 LST. Photochemical process was a major contributor to the NO_2 diurnal changes, with the peak process rate as high as 152.5 ppb/hour. Emission and chemistry are two major processes driving the NO concentration changes at this site, with emission providing NO and chemistry consuming NO immediately after it emitted (Table 5). This indicates that although the NO_2 predicted concentrations can get closer to the observations at some hours of the day by increasing NOx emissions, the model still could not capture the NO_2 temporal changes as observed. The magnitudes of NOx emissions are not the only problems in the model.

Sillman ratio analysis is also conducted on the emission sensitivity run s2. Figure 12 shows the Sillman ratio plot at KHAF and BANI sites on July 03, 2007 for the sensitivity run s2. Comparing with the original model run, we can see that the Sillman

ratio at these two sites decreased significantly - the value is much lower than 0.5 throughout the day, indicating the system is under NOx-inhibited condition.

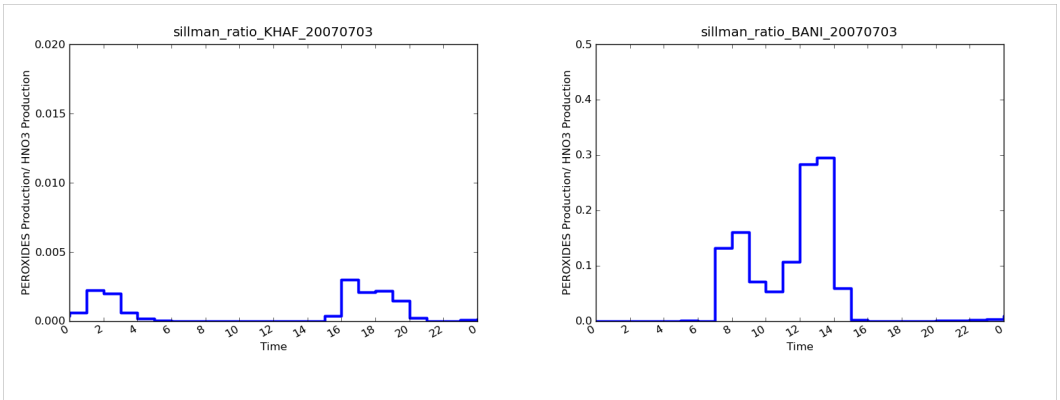

Fig. 12 Sillman ratio for KHAF and BANI sites on July 03, 2007 in the sensitivity run s2.

CHAPTER IV

SUMMARY AND CONCLUSIONS

Model predictions for O_3 and NO_2 were evaluated against ground level hourly observations in the UAE. The results indicate severe over-prediction of O_3 and under-prediction of NO_2 especially in the Abu Dhabi urban region. We used process analysis to understand physical and chemical processes underlying the formation of high ozone concentrations in the model. According to the process analysis results, chemistry plays an important role for ozone presence in UAE in the model, especially for the Abu Dhabi urban region. The photochemical processes rates at the urban site KHAF is much higher than the ones at the rural site LIWA. Sillman ratio analysis indicates that both of KHAF and LIWA sites are under NOx-limited conditions in the original model run.

Our results also show that advection process is another major contributor to ozone and the diurnal changes for the ozone precursors in UAE. For air pollution control strategies, we should pay attention to not only the local emissions of ozone precursors such as NOx and VOC, but also the long-range transport from the surrounding area. More accurate meteorological simulation such as better predictions of wind speeds and wind directions can also partially improve ozone predictions.

The problem of missing emissions from mobile sources at the urban region of Abu Dhabi indicates the disadvantage of using UAE main roads as a spatial surrogate for emission spatial distribution. By adding emissions to the cell where emissions were missing in the original model simulation and increasing the magnitudes of the NOx in

the Abu Dhabi urban region, we still had difficulty to fit the predicted O_3 and NO_2 to the observed values for the whole diurnal cycle in the selected high ozone days. This suggests the need of further investigation on not only the spatial allocation and the magnitudes but also the temporal profile of the emissions.

The significant changes in the sensitivity run s2 indicate that the model is very sensitive to NOx emissions. Through increasing NOx emissions rates in the model, we have seen significant predicted O_3 concentrations decrease. Compared with the original model simulation, the sensitivity run s2 causes predicted hourly O_3 concentrations to decrease by up to 80 ppb. The system also switched from NOx-limited condition, with the peak Sillman-ratio of 3.8 at KHAF on July 03 in the original run, to NOx-inhibited condition, with the peak Sillman-ratio of 0.003 at KHAF on the same day in the sensitivity run s2.

Despite high observations reported in several other studies in the UAE, such as satellite observations from Ozone Monitoring Instrument (OMI) and Scanning Imaging Absorption Spectrometer for Atmospheric CHartographY (SCIAMACHY), monitoring data from the EAD network did not record a single 1-hour average ozone concentration in 2007 that exceeded the EAD standard. This raises questions about whether the measurements accurately reflect the exposure of the population in the UAE. The lack of violations could be due to the placement of the monitors or integrity of the data. The surface observational data used in this study are considered to be uncertain because no documentation of QA/QC methods and procedures can be provided for data quality evaluation by Jacques Whitford Group who operated the air monitoring stations during years 2007-2008.

The uncertainties in the model simulations could be another reason for the high discrepancy between the ozone predictions and the suppressed ozone observations. One hypothesis is that ozone is being destroyed by reaction with fresh NO emissions,

while not enough NO emissions were input into the model because of lack of local emissions source data in the UAE. This hypothesis is supported by the significant O_3 concentrations decrease by increasing anthropogenic NOx emissions and switching the system into NOx-inhibited condition in the sensitivity run s2 in our study.

The PM_{10} observational data from air quality monitoring network shows that this country is under enhanced burden of dust, with observed PM_{10} severely exceeding the emirate standards at each site. A second hypothesis would suggest that dust influences ozone formation by two processes: decreasing the transmission of sunlight to the surface, thereby reducing ozone formation, and by destroying ozone by directly reactions on the surface of particulate matter, a process that is not well understood but may be particularly important because of the widespread dust in the Middle East ([32]; [33]). A recent study shows aerosols can lead to about 2-17% surface ozone reduction in the urban area of Mexico City, larger reductions during early morning hours[34]. Including effects of dust on ozone can be one of the recommendations for improvement of model performance and we can implement this finding into our model simulation in the future.

REFERENCES

1. Business Monitor International Ltd, chapter 3: 10-Year Forecast. UAE Business Forecast Report, 2009: p. 27-28.

2. Lippmann, M., Health effects of tropospheric ozone: review of recent research findings and their implications to ambient air quality standards. J Expo Anal Environ Epidemiol, 1993. 3(1): p. 103-29.

3. Krishna, M.T., et al., Effects of 0.2 ppm ozone on biomarkers of inflammation in bronchoalveolar lavage fluid and bronchial mucosa of healthy subjects. Eur Respir J, 1998. 11(6): p. 1294-300.

4. Li, Q.B., et al., A tropospheric ozone maximum over the Middle East. Geophysical Research Letters, 2001. 28(17): p. 3235-3238.

5. Liu, J.J., et al., Analysis of the summertime buildup of tropospheric ozone abundances over the Middle East and North Africa as observed by the Tropospheric Emission Spectrometer instrument. J. Geophys. Res., 2009. 114(D5): p. D05304.

6. Lelieveld, J., et al., Severe ozone air pollution in the Persian Gulf region. Atmospheric Chemistry and Physics, 2009. 9(4): p. 1393-1406.

7. Duncan, B.N., et al., The influence of European pollution on ozone in the Near East and northern Africa. Atmospheric Chemistry and Physics, 2008. 8(8): p. 2267-2283.

8. West, J.J., et al., Effect of regional precursor emission controls on long-range ozone transport - Part 1: Short-term changes in ozone air quality. Atmospheric Chemistry and Physics, 2009. 9(16): p. 6077-6093.

9. West, J.J., et al., Effect of regional precursor emission controls on long-range ozone transport - Part 2: Steady-state changes in ozone air quality and impacts on human mortality. Atmospheric Chemistry and Physics, 2009. 9(16): p. 6095-6107.

10. Anenberg, S.C., et al., Intercontinental Impacts of Ozone Pollution on Human Mortality. Environmental Science & Technology, 2009. 43(17): p. 6482-6487.

11. Weinroth, E., et al., Simulations of Mideast transboundary ozone transport: A source apportionment case study. Atmospheric Environment, 2008. 42(16): p. 3700-3716.

12. Abdul-Wahab, S.A., C.S. Bakheit, and S.M. Al-Alawi, Principal component and multiple regression analysis in modelling of ground-level ozone and factors affecting its concentrations. Environmental Modelling & Software, 2005. 20(10): p. 1263-1271.

13. Ajjaji, R., A.A. Al-Katheri, and K. Al-Chergui. Evaluation of United Arab Emirates WRF two-way nested model on a set of thick coastal fog situations. in WRF Users Conference. 2007. Boulder, CO.

14. Ajjaji, R., A.A. Al-Katheri, and A. Dhanhani. Implementation and preliminary tests of an air quality forecasting system based on WRF-Chem over Middle-East, Arabian Peninsula and United Arab Emirates. in WRF Users Conference. 2007. Boulder, CO.

15. Wheeler, N.J.M. and S.B. Reid, Photochemical Modeling of an Industrial City in Qatar, 2006, Sonoma Technology, Inc.: Petaluma, CA.

16. Byun, D. and K.L. Schere, Review of the governing equations, computational algorithms, and other components of the models-3 Community Multiscale Air Quality (CMAQ) modeling system. Applied Mechanics Reviews, 2006. 59(1-6): p. 51-77.

17. Byun, D. and J.K.S. Ching, Science Algorithms of the EPA Models-3 Community Multiscale Air Quality (CMAQ) Modeling System, 1999, U.S. EPA.

18. Yarwood, G., et al., Updates to the Carbon Bond Chemical mechanism: CB05. Final Report to the US EPA, 2005, ENVIRON Inc.

19. Gery, M.W., et al., A Photochemical Kinetics Mechanism for Urban and Regional Scale Computer Modeling. J. Geophys. Res., 1989. 94(D10): p. 12925-12956.

20. Aijun Xiu, N.D., Adel Hanna, Uma Shankar, Zac Adelman, Sarav Arunachalam, Jason West, Will Vizuete, Ken Sexton, <Meteorological Modeling over the United Arab Emerites in support of Air Quality Modeling.pdf>. In press

21. Skamarock, W.C., Klemp, Joseph B., Dudhia Jimy, Grill David O., et al., , A Description of the Advanced Research WRF Version 3. NCAR Technical Note, 2008.

22. Zachariah Adelman, L.R., Mohammad Omary, Uma Shankar <Developing Emissions for Multi-pollutant Air Quality Modeling in the Middle East.pdf>. 2011.

23. Shi, C., H.J.S. Fernando, and J. Yang, Contributors to ozone episodes in three U.S./Mexico border twin-cities. Science of The Total Environment, 2009. 407(18): p. 5128-5138.

24. Khiem, M., et al., Process analysis of ozone formation under different weather conditions over the Kanto region of Japan using the MM5/CMAQ modelling system. Atmospheric Environment, 2010. 44(35): p. 4463-4473.

25. Jang, J.-C.C., H.E. Jeffries, and S. Tonnesen, Sensitivity of ozone to model grid resolution -- II. Detailed process analysis for ozone chemistry. Atmospheric Environment, 1995. 29(21): p. 3101-3114.

26. EMEP, European Monitoring and Evaluation Programme 2010.

27. EPA, Guidance on the Use of Models and Other Analyses for Demonstrating Attainment of Air Quality Goals for O3, PM and Regional Haze., 2007, EPA.

28. Russell, A. and R. Dennis, NARSTO critical review of photochemical models and modeling. Atmospheric Environment, 2000. 34(12-14): p. 2283-2324.

29. Arunachalam Saravanan, A.Z., Mathur Rohit A Comparison of Models-3/CMAQ and the MAQSIP modeling systems for Ozone Modeling in North Carolina. 2001.

30. Sillman, S., The use of NOy, H2O2, and HNO3 as indicators for ozone-NOx-hydrocarbon sensitivity in urban locations. Journal of Geophysical Research 1995. 100(D7): p. 14175-14188.

31. Xie Ying, L.B., Jobson Tom, VOC/NOX SENSITIVITY ANALYSIS FOR OZONE PRODUCTION USING CMAQ PROCESS ANALYSIS FOR THE PACIFIC NORTHWEST. the 6th Annual CMAS Conference, Chapel Hill, NC, 2007.

32. Bian, H.C.S.Z., Heterogeneous impact of dust on tropospheric ozone: Sensitivity to season, species, and uptake rates. J. Geophys. Res. Atm., 2003.

33. Mogili, P.K., et al., Heterogeneous Uptake of Ozone on Reactive Components of Mineral Dust Aerosol:‚Äâ An Environmental Aerosol Reaction Chamber Study. The Journal of Physical Chemistry A, 2006. 110(51): p. 13799-13807.

34. Li, G., et al., Aerosol effects on the photochemistry in Mexico City during MCMA-2006/MILAGRO campaign. Atmos. Chem. Phys., 2011. 11(11): p. 5169-5182.